Thermal conductance in a two-slit quantum waveguide*

Nie Liu-Ying(聂六英)†, Li Chun-Xian(李春先), Zhou Xiao-Ping(周晓萍), Wang Cheng-Zhi(王成志), and Cheng Fang(程 芳)

School of Physics and Electronic Science, Changsha University of Science and Technology, Changsha 410114, *China*

(Received 21 May 2011; revised manuscript received 30 August 2011)

Using the scattering-matrix method, we investigate the thermal conductance in a two-slit quantum waveguide at low temperature. The results show that the total thermal conductance decreases monotonically with temperature increasing. Moreover, we find that the behaviours of the thermal conductance versus temperature are different for different types of slits.

Keywords: acoustic phonon transport, thermal conductance, quantum wire

PACS: 63.22.–m, 44.10.+i, 73.23.Ad **DOI:** 10.1088/1674-1056/21/2/026301

1. Introduction

In recent years, extensive attention has been paid to the thermal transport associated with a set of discrete acoustic phonon modes in semiconductor nanostructures and nanoscale devices in which the wavelength of phonon is comparable to or larger than the structure feature size. It is known that low-temperature thermal transport properties of nanostructure can be very different from the corresponding bulk properties because the phonon is scattered elastically but not inelastically in the mesoscopic regime. The thermal conductance associated with acoustic phonons were reported in various kinds of nanostructures such as superlattices,[1−4] thin films,[5−8] nanowires,[9−17] and nanotubes.[18−20] Rego and Kirzemow[21] predicted the existence of a universal quantum of the thermal conductance in the dielectric quantum wire at low enough temperature using the Landauer formulation of transport theory. The universal thermal conductance was observed in a suspended silicon nitride bridge.[22] However, the universal thermal conductance was not observed as the temperature increases in a range from 0.08 K to 0.2 K. It is known now that the discontinuity can lead to additional scattering of transport phonon and result in the decrease of the thermal conductance. Santamore and Cross[23,24] investigated the effect of surface roughness on the universal thermal conductance in a dielectric quantum wire at low temperature. Acoustic phonon transport and thermal conductance were investigated in various quantum wire structures such as nanowires with abrupt junction,[25,26] with structural defects,[27,28] with stub structure,[29−35] and with catenoidal contacts.[36]

In the present study, we investigate thermal transport properties of semiconductor nanostructure shown in Fig. 1. For simplicity, we assume that each region has the same thickness and the thickness is small with respect to the other dimensions and also to the wavelength of the elastic waves. In such a system there exist three types of acoustic modes: longitudinal polarized P mode, vertically polarized SV mode and horizontally polarized shear SH mode. It is known that at very low temperature the lowest vibrational modes include four types of acoustic modes (namely the dilatational, torsional and two types of flexural modes) and two types of optical modes (namely two shear modes) in a three-dimensional (3D) quantum structure. However, for a two-dimensional (2D) quantum structure where the thickness of the sample is much less than the assumed width, the lowest vibrational

*Project supported by the Natural Science Foundation of Hunan Province of China (Grant No. 09JJ5005) and the National Natural Science Foundation of China (Grant Nos. 10947134 and 11004017).

†Corresponding author. E-mail: nieliuying@163.com

© 2012 Chinese Physical Society and IOP Publishing Ltd

modes can be classified as three types of modes, namely SH, SV and P modes. The latter is considered in this paper. Their polarization directions are along x, y and z directions, respectively. The horizontally polarized shear SH mode is decoupled from the P or SV mode polarized in x–y plane. At a low temperature, the effect of mode mixing on the thermal conductance is very small and the thermal conductance of the SH wave has similar features to those of the P (or SV) mode. So in the present paper, we only discuss the thermal conductance of SH mode. The results show some interesting physical effects: (i) it is possible that thermal conductance becomes very small at its minimum; (ii) there is a qualitative difference in the dependence of the thermal conductance on slit width.

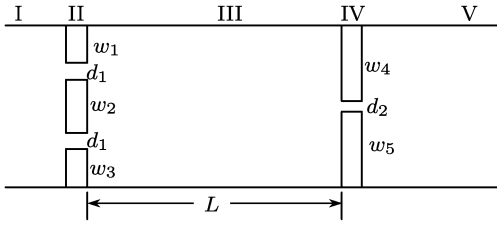


Fig. 1. Schematic illustration of a two-slit quantum waveguide. The structure is divided into five regions. Regions I and V are semi-infinite incident and outgoing leads, respectively. Two identical slits each with width $d_1$exist in region II. The analysis slit with width d_2 exists in region IV. The length L of region III represents the distance between two-slit and analysis slit. Notice that w_1–w_5 denote the widths of obstacles, respectively.

The rest of the present paper is organized as follows. In Section 2, we give a brief description of the model and the formulas to be used in calculations. The calculated results are presented in Section 3 together with analyses. Finally, a summary is made in Section 4.

2. Model and formalism

We consider the model structure shown in Fig. 1. For the structure considered here, the formula for the thermal conductance can be expressed as

$$K = \frac{\hbar^2}{\kappa_B T^2} \sum_m \frac{1}{2\pi} \int_{\omega_m}^{\infty} \tau_m(\omega) \frac{\omega^2 \, \mathrm{e}^{\beta\hbar\omega}}{(\mathrm{e}^{\beta\hbar\omega} - 1)^2} \mathrm{d}\omega. \quad (1)$$

Here, $\tau_m(\omega)$ is the energy transmission coefficient from mode m of region I at frequency ω across all the interfaces into the modes of region V; ω_m is the cutoff frequency of the m-th mode; $\beta = 1/k_{\mathrm{B}}T$, with k_{B} being the Boltzman constant and T the temperature; and $\hbar$ is the Planck's constant. The effect of scattering is introduced through the transmission coefficient, $\tau_m(\omega)$. In this paper, we employ the elastic model to calculate the transmission coefficient of acoustic phonon. In the elastic approximation, the elastic equation of motion for SH wave is

$$\frac{\partial^2 \psi}{\partial t^2} - v^2 \nabla^2 \psi = 0, \quad (2)$$

where v is the sound velocity of SH mode, related to the mass density ρ and elastic stiffness constant C_{44} by

$$v^2 = C_{44}/\rho. \quad (3)$$

The solutions to Eq. (2) in different regions can be written as

$$\Psi^{\alpha}(x,y) = \sum_{m_1=0}^{N_1} \left[A^{\alpha}_{m_1} \, \mathrm{e}^{\mathrm{i}k^{\alpha}_{m_1} x} + B^{\alpha}_{m_1} \, \mathrm{e}^{-\mathrm{i}k^{\alpha}_{m_1} x} \right] \times \phi^{\alpha}_{m_1}(y) \quad (\alpha = \mathrm{I},\ \mathrm{III},\ \mathrm{V}) \quad (4)$$

in region α, where $\phi^{\alpha}_{m_1}(y)$ represents the transverse wave function of acoustic mode m in region α. The transverse wave function of acoustic mode is

$$\phi^{\alpha}_{m_1}(y) = \begin{cases} \sqrt{\dfrac{2}{w_1 + w_2 + w_3 + 2d_1}} \cos \dfrac{m_1 \pi}{w_1 + w_2 + w_3 + 2d_1} y & (m \neq 0), \\ \sqrt{\dfrac{1}{w_1 + w_2 + w_3 + 2d_1}} & (m = 0). \end{cases} \quad (5)$$

And $k^{\alpha}_{m_1}$ can be given by the energy conservation condition as

$$k^{\alpha}_{m_1} = \sqrt{\frac{\omega^2}{v_I^2} - \frac{m_1^2 \pi^2}{(w_1 + w_2 + w_3 + 2d_1)^2}}, \quad (6)$$

where ω is the incident phonon frequency. For region II, we have

$$\Psi^{\mathrm{II}}(x,y) = \sum_{m_2=0}^{N_2} \left[C^A_{m_2} \, \mathrm{e}^{\mathrm{i}k^A_{m_2} x} + D^A_{m_2} \, \mathrm{e}^{-\mathrm{i}k^A_{m_2} x} \right] \phi^A_{m_2}(y) + \sum_{m_2=1}^{N_2} \left[C^B_{m_2} \, \mathrm{e}^{\mathrm{i}k^B_{m_2} x} + D^B_{m_2} \, \mathrm{e}^{-\mathrm{i}k^B_{m_2} x} \right] \phi^B_{m_2}(y). \quad (7)$$

The transversal wave functions $\phi^A_{m_2}(y)$ and wave number $\kappa^A_{m_2}$ and $\phi^B_{m_2}(y)$ and $\kappa^B_{m_2}$ should be expressed as

$$\phi^A_{m_2}(y) = \begin{cases} \sqrt{\dfrac{2}{d_1}} \cos \dfrac{m_2\pi}{d_1}(y - w_1 - w_2 - d_1) \ \ (m_2 \neq 0), \\ \sqrt{\dfrac{1}{d_1}} \ \ (m_2 = 0), \end{cases} \tag{8}$$

for $w_1 + w_2 + d_1 \leq y \leq w_1 + w_2 + 2d_1$,

$$k^A_{m_2} = \sqrt{\frac{\omega^2}{v_A^2} - \frac{m_2^2\pi^2}{d_1^2}}; \tag{9}$$

$$\phi^B_{m_2}(y) = \begin{cases} \sqrt{\dfrac{2}{d_1}} \cos \dfrac{m_2\pi}{d_1}(y - w_1) \ \ (m_2 \neq 0), \\ \sqrt{\dfrac{1}{d_1}} \ \ (m_2 = 0), \end{cases} \tag{10}$$

for $w_1 \leq y \leq w_1 + d_1$ and

$$k^B_{m_2} = \sqrt{\frac{\omega^2}{v_{\rm B}^2} - \frac{m_2^2\pi^2}{d_1^2}}. \tag{11}$$

In region IV, the solution in Eq. (2) can be written as

$$\psi^{\rm III}(x, y) = \sum_{m_3=0}^{N_1} \left(A^{\rm III}_{m_3} \, {\rm e}^{{\rm i}k^{\rm III}_{m_3}x} + B^{\rm III}_{m_3} \, {\rm e}^{-{\rm i}k^{\rm III}_{m_3}x} \right) \phi^{\rm III}_{m_3}(y). \tag{12}$$

The relation between the coefficients in any two adjacent regions can be obtained by the use of the scattering matrix method. We assume that the scattering matrix at the interface $x = 0$ is $S^{\rm I}$. Then we have

$$\begin{pmatrix} B^{\rm I} \\ C^A \\ C^B \end{pmatrix} = S^{\rm I} \begin{pmatrix} A^{\rm I} \\ D^A \\ D^B \end{pmatrix}. \tag{13}$$

The scattering matrix $S^{\rm I}$ can be derived from the boundary conditions at interfaces: the displacement $\psi(x, y)$ and the force $C_{11}\psi'(x, y)$ should be continuous at each interface. Similarly, we can obtain the scattering matrix $S^{\rm II}$ in the region II and $S^{\rm III}$ at the interface.

By using the scattering matrix cascading method, the total scattering matrix S of the quantum structure can be constructed through the composition of the individual scattering matrices as

$$S = S^{\rm I} \otimes S^{\rm II} \otimes S^{\rm III}. \tag{14}$$

In the calculations, we will employ those values of dielectric constants and density of GaAs and AlAs: $C_{44}({\rm GaAs}) = 5.99$ $(10^{10}$ ${\rm N \cdot m^{-2}})$ and $\rho({\rm GaAs}) = 5317.6$ $({\rm kg \cdot m^{-3}})$.

3. Numerical results and discussion

We first show in Fig. 2 the dependences of the thermal conductance divided by the temperature reduced by the zero-temperature universal $\pi^2\kappa_{\rm B}^2 T/3h$ on reduced temperature $\kappa_{\rm B}T/\hbar\Delta$ for different values of width L in the structure as depicted in Fig. 1. Here, $\Delta = \omega_{m+1} - \omega_m = \pi v_{\rm SH}/\omega$, ($v_{\rm SH}$ is the acoustic wave velocity in region I) denotes the splitting of the cutoff frequency between the $(m+1)$-th and m-th modes in region I. Figures 2(a) and 2(b) correspond to the reduced thermal conductances of modes 0 and 1 respectively and figure 2(c) corresponds to the total thermal conductance. Note that the total thermal conductance includes the contributions of the first six modes. The dotted, dashed and solid curves correspond to $L = 100$ nm, 80 nm, and 60 nm, respectively. From Fig. 2(a), it can be found that with the increase of temperature, the reduced thermal conductance K/T of zero mode is always decreasing, which approaches the ideal universal value $\pi^2\kappa_{\rm B}^2 T/3h$ as the temperature $T \to 0$. Moreover, we can clearly see that with the increase of width L, the thermal conductance varies very little. We also find from Fig. 2(b) that the value K/T of modes 1 is small. It is found from Fig. 2(c) that the thermal conductance decreases monotonically with temperature increasing. In such cases, it is possible that thermal conductance becomes very small at its minimum. The results can be understood from physical view. The coupling strength can be expressed by the overlap of the transverse functions of the incident wave and the excited wave. For region I and region II, the coupling strength is expressed as $\int \phi^{\rm I}_{m_1}\phi^A_{m_2}\,{\rm d}y$ and $\int \phi^{\rm I}_{m_1}\phi^B_{m_2}\,{\rm d}y$ respectively. According to Eqs. (5), (8), and (10), the coupling strength is small when d_1 is small. The weaker the coupling between region I and region II, the smaller the value K/T of total thermal conductance through the junction will be, which is also true for region III and region IV.

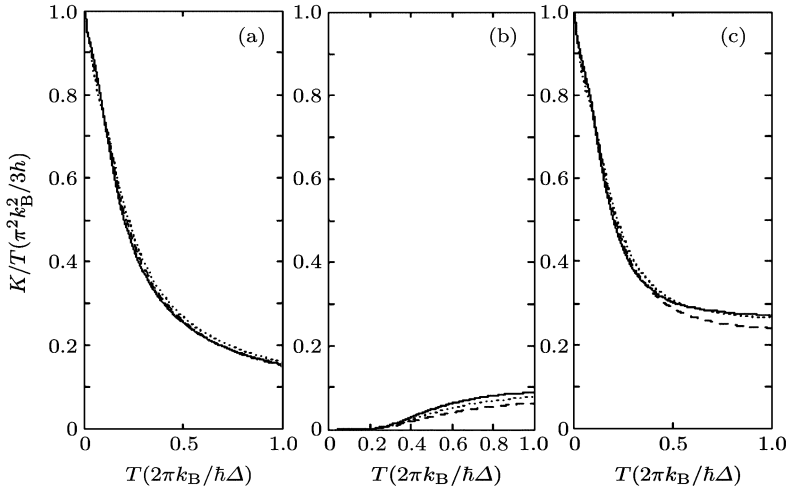


Fig. 2. Thermal conductances divided by temperature, K/T, which is reduced by the zero-temperature universal value $\pi^2\kappa_B^2 T/3h$, each as a function of the reduced temperature $\kappa_B T/\hbar\Delta$, for different values of width L. Panels (a) and (b) correspond to K/T values of modes 0 and 1 respectively and panel (c) corresponds to the total K/T. The dotted, dashed and solid curves correspond to $L = 100$, 80 and 60 nm respectively.

In Fig. 3, we investigate the dependences of the reduced thermal conductance on the reduced temperature for different values of width d_1. The dotted, dashed and solid curves correspond to $d_1 = 1$ nm, 3 nm and 5 nm, respectively. It is clearly observed that for different values of width d_1 of slit the difference between their thermal conductances is very small. However, this does not always happen to all the slits in the structure. We now turn our study to the influence of analysis slit on the thermal conductance. Figure 4 shows the reduced total thermal conductance versus the width d_2 of analysis slit. From Fig. 4, we can see clearly that the reduced thermal conductance changes with width d_2. The longer the width d_2 is, the bigger the value K/T within the region examined will be. The dependence of the thermal conductance on the reduced temperature for width d_1 is different from that for width d_2, which results from the different coupling effects and interference effects. When the incoming wave enters into region III, it partly goes into the analysis slit and partly is reflected back. The interference of reflected wave with the incoming wave takes place in region III. However, when the incoming wave enters into region V, there is no reflection. As the width d_1 of slit increases, the stronger scattering due to discontinuous interfaces results in the decrease of the thermal conductance. However, mode–mode coupling results in the increase of the thermal conductance. This will induce a nonlinear behaviour of the thermal conductance. When the width d_2 of slit increases, there is no reflection in region V, the mode–mode coupling results in the increase of thermal conductance.

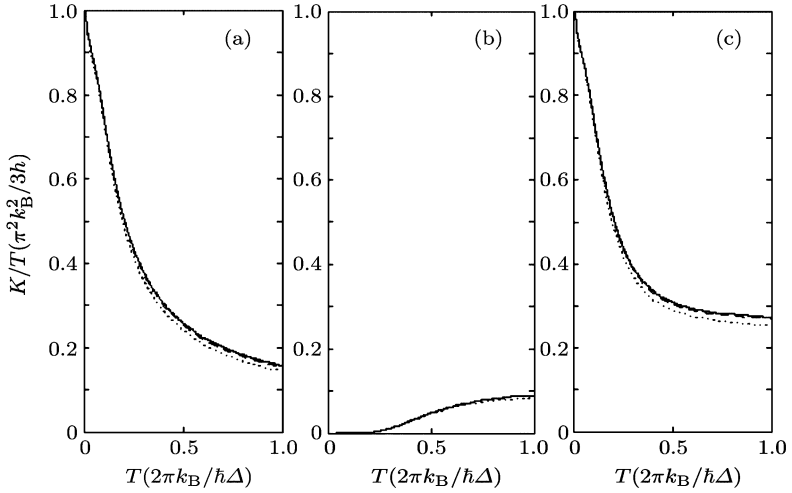


Fig. 3. Thermal conductances divided by temperature, K/T, which is reduced by the zero-temperature universal value $\pi^2\kappa_B^2 T/3h$, each as a function of the reduced temperature $\kappa_B T/\hbar\Delta$, for different width d_1. Panels (a) and (b) correspond to K/T values of modes 0 and 1 respectively and panel (c) corresponds to total K/T. The dotted, dashed and solid curves correspond to $d_1 = 1$, 3 and 5 nm respectively.

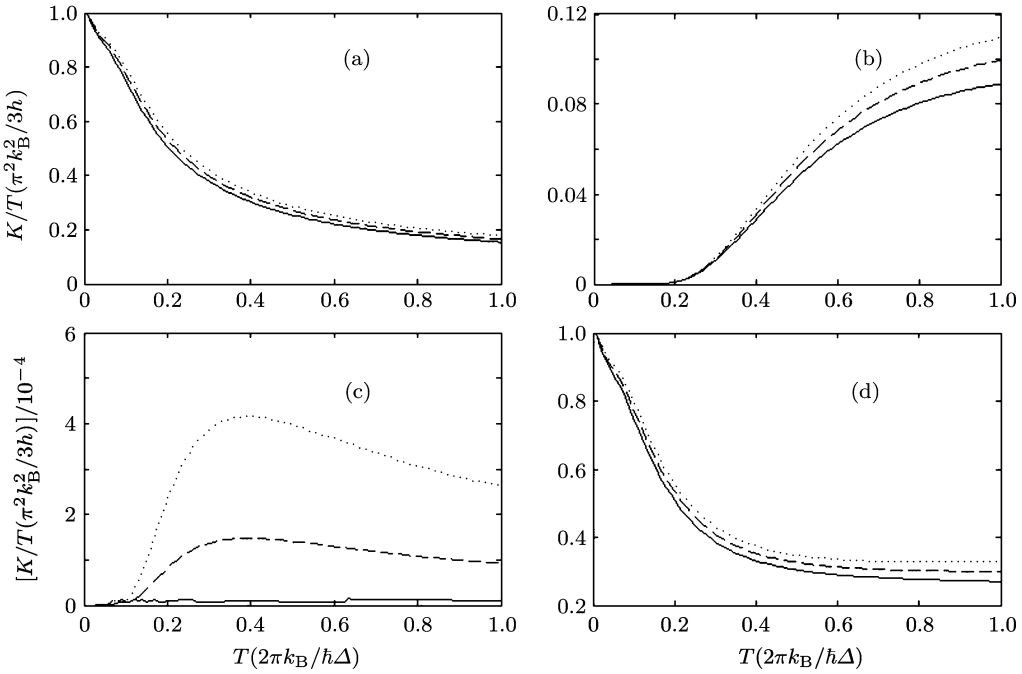


Fig. 4. Thermal conductances divided by temperature, K/T, which is reduced by the zero-temperature universal value $\pi^2\kappa_B^2T/3h$, each as a function of the reduced temperature $\kappa_BT/\hbar\Delta$, for different values of width d_2. Panels (a)–(c) correspond to K/T values of modes 0, 1 and 2, respectively and panel (d) corresponds to total K/T. The dotted, dashed and solid curves correspond to $d_2 = 6$, 4 and 2 nm respectively.

To explore the effect of the position of the analysis slit in nanowire on K/T, figure 5 displays the K/T values, each as a function of the reduced temperature, for different values of ratio $w_4 : w_5$. Figures 5(a)–5(c) correspond to the reduced thermal conductances of modes 0, 1 and 2, respectively. The dotted, dashed, and solid curves correspond to $w_4 : w_5 = 1 : 1$, $1 : 3$, and $1 : 9$ respectively. Here, we fix $w_4 + w_5 = 98$ nm, $d_2 = 2$ nm. From Figs. 5(a), 5(b), and 5(d), it is clearly seen that when the analysis slit is in the middle of the quantum wire, the K/T value is the biggest for the thermal conductance. Here, it should be noted, in particular, that the thermal conductances are similar in characteristics for the Young's two-slit experiment.

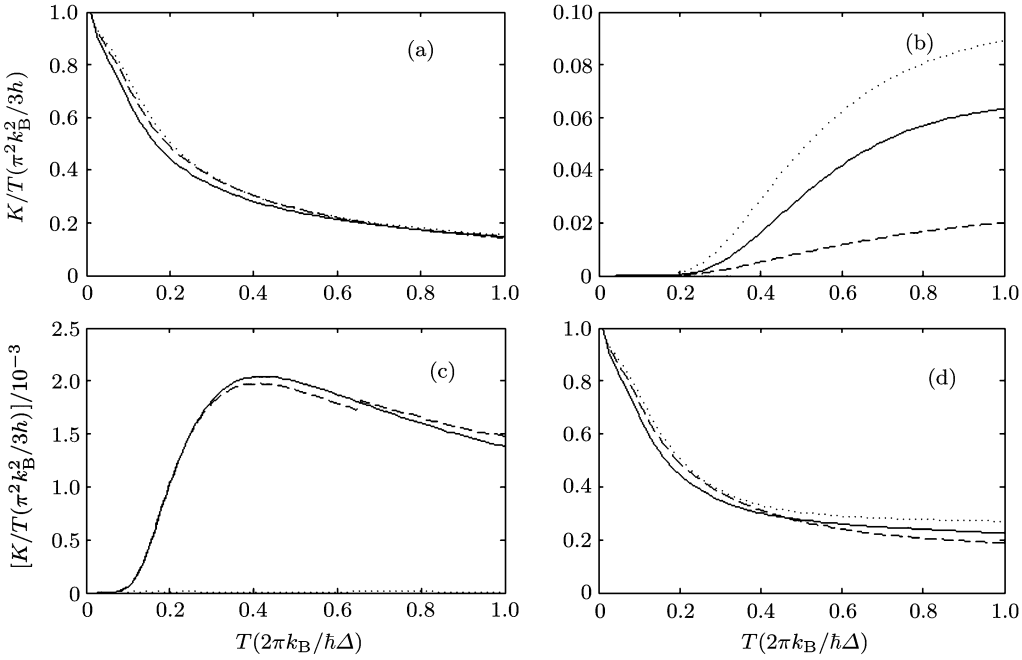


Fig. 5. Values of total K/T, each as a function of the reduced temperature $\kappa_BT/\hbar\Delta$, for different values of ratio $w_4 : w_5$. Panels (a)–(c) correspond to K/T values of modes 0, 1 and 2, respectively and panel (d) corresponds to total K/T. The dotted, dashed and solid curves correspond to $w_4 : w_5 = 1 : 1$, $1 : 3$ and $1 : 9$ respectively.

However, the thermal conductance is unlike the case of two-slit electronic waveguides. This is due to the fact that the acoustic phonon satisfies the stress-free boundary condition, whereas the electron satisfies the hardwall boundary condition. For electron transport, when the energy of the incident electron is lower than the threshold energy, the electron cannot propagate through the structure. However, for acoustic phonon transport, the stress-free boundary condition allows the mode with $\omega \to 0$ to propagate in the structure.

4. Summary

In the present study, we investigated the thermal conductance in a two-slit quantum waveguide using scattering-matrix method. We observed some novel and interesting characteristics for thermal conductance in the structure. We found that the total thermal conductance which includes the contribution of the first six propagating modes decreases monotonically with temperature increasing. In such cases, it is possible that the thermal conductance becomes very small at its minimum. The K/T value of mode 1 is small and the K/T value of mode 2 is close to zero. We also noticed that there is a qualitative difference in the dependence of the thermal conductance on slit width. For different values of width d_1 of the slit, the difference between their thermal conductances is very small. For different values of width d_2 of the slit, the difference between their thermal conductances is obvious.

References

[1] Lee S M, Cahill D G and Venkatasubramanian R 1997 *Appl. Phys. Lett.* **70** 2957

[2] Chen G 1998 *Phys. Rev.* B **57** 14958

[3] Bies W E, Radtke R J and Ehrenreich H 2000 *J. Appl. Phys.* **88** 1498

[4] Simkin M V and Mahan G D 2000 *Phys. Rev. Lett.* **84** 927

[5] Yu X Y, Chen G, Verma A and Smith J S 1995 *Appl. Phys. Lett.* **67** 3554

[6] Balandin A and Wang K L 1998 *Phys. Rev.* B **58** 1544

[7] Philip J, Hess P, Feygelson T, Butler J E, Chattopadhyay S, Chen K H and Chen L C 2003 *J. Appl. Phys.* **93** 2164

[8] Yang P, Wu Y S, Xu H F, Xu X X, Zhang L Q and Li P 2011 *Acta Phys. Sin.* **60** 066601 (in Chinese)

[9] Tighe T S, Worlock J M and Roukes M L 1997 *Appl. Phys. Lett.* **70** 2687

[10] Chen G 2000 *Int. J. Thermal Sci.* **39** 471

[11] Chen G and Zeng T 2001 *Microstructure Thermophysical Engineering* **5** 71

[12] Glavin B A 2001 *Phys. Rev. Lett.* **86** 4318

[13] Volz S, Lemonnier D and Saulnier J B 2001 *Microstructure Thermophysical Engineering* **5** 191

[14] Zou J and Balandin A 2001 *J. Appl. Phys.* **89** 2932

[15] Huang W Q, Chen K Q, Shuai Z, Wang L L and Hu W Y 2005 *Phys. Lett.* A **336** 245

[16] Ye F Q, Li K M and Peng X F 2011 *Acta Phys. Sin.* **60** 036806 (in Chinese)

[17] Li H B and Li Z 2010 *Chin. Phys.* B **19** 054401

[18] Kim P, Shi L, Majumdar A and McEuen P L 2001 *Phys. Rev. Lett.* **87** 215502

[19] Hou Q W, Cao B Y and Guo Z Y 2009 *Acta Phys. Sin.* **58** 7809 (in Chinese)

[20] Wang J L, Xiong G P, Gu M, Zhang X and Liang J 2009 *Acta Phys. Sin.* **58** 4536 (in Chinese)

[21] Rego L G C and Kirczenow G 1998 *Phys. Rev. Lett.* **81** 232

[22] Schwab K, Henriksen E A, Worlock J M and Roukes M L 2000 *Nature* (London) **404** 974

[23] Santamore D H and Cross M C 2001 *Phys. Rev. Lett.* **87** 115502

[24] Santamore D H and Cross M C 2001 *Phys. Rev.* B **63** 184306

[25] Li W X, Chen K Q, Duan W H, Wu J and Gu B L 2003 *J. Phys.* D: *Appl. Phys.* **36** 3027

[26] Chang C M and Geller M R 2005 *Phys. Rev.* B **71** 125304

[27] Chen K Q, Li W X, Duan W H, Shuai Z and Gu B L 2005 *Phys. Rev.* B **72** 045422

[28] Nie L Y, Wang L L, Zhao L H, Huang W Q, Tang L M, Wang X J and Chen K Q 2006 *Phys. Lett.* A **359** 234

[29] Li W X, Chen K Q, Duan W H, Wu J and Gu B L 2004 *J. Phys.*: *Condens. Matter* **16** 5049

[30] Huang W Q, Chen K Q, Shuai Z, Wang L L, Hu W Y and Zou B S 2005 *J. Appl. Phys.* **98** 093524

[31] Tang L M, Wang L L, Chen K Q, Huang W Q and Zou B S 2006 *Appl. Phys. Lett.* **88** 163505

[32] Yang P, Sun Q F, Guo H and Hu B B 2007 *Phys. Rev.* B **75** 235319

[33] Peng X F, Chen K Q, Zou B S and Zhang Y 2007 *Appl. Phys. Lett.* **90** 193502

[34] Xie F, Chen K Q, Wang Y G and Zhang Y 2008 *J. Appl. Phys.* **103** 084501

[35] Xie F, Chen K Q, Wang Y G and Zhang Y 2008 *J. Appl. Phys.* **104** 054312

[36] Peng X F, Chen K Q, Wan Q, Zou B S and Duan W H 2010 *Phys. Rev.* B **81** 195317